Restructuring of the Gut Microbiome by Intermittent Fasting Prevents Retinopathy and Prolongs Survival in *db/db* Mice

Eleni Beli,[1] Yuanqing Yan,[2] Leni Moldovan,[3] Cristiano P. Vieira,[4] Ruli Gao,[5] Yaqian Duan,[6] Ram Prasad,[4] Ashay Bhatwadekar,[7] Fletcher A. White,[8] Steven D. Townsend,[9] Luisa Chan,[10] Caitlin N. Ryan,[10] Daniel Morton,[10] Emil G. Moldovan,[11] Fang-I Chu,[12] Gavin Y. Oudit,[13] Hartmut Derendorf,[14] Luciano Adorini,[15] Xiaoxin X. Wang,[16] Carmella Evans-Molina,[1,6,17] Raghavendra G. Mirmira,[1,6,17] Michael E. Boulton,[4] Mervin C. Yoder,[1] Qiuhong Li,[18] Moshe Levi,[16] Julia V. Busik,[19] and Maria B. Grant[4]

Diabetes 2018;67:1867–1879 | https://doi.org/10.2337/db18-0158

Intermittent fasting (IF) protects against the development of metabolic diseases and cancer, but whether it can prevent diabetic microvascular complications is not known. In *db/db* mice, we examined the impact of long-term IF on diabetic retinopathy (DR). Despite no change in glycated hemoglobin, *db/db* mice on the IF regimen displayed significantly longer survival and a reduction in DR end points, including acellular capillaries and leukocyte infiltration. We hypothesized that IF-mediated changes in the gut microbiota would produce beneficial metabolites and prevent the development of DR. Microbiome analysis revealed increased levels of Firmicutes and decreased Bacteroidetes and Verrucomicrobia. Compared with *db/db* mice on ad libitum feeding, changes in the microbiome of the *db/db* mice on IF were associated with increases in gut mucin, goblet cell number, villi length, and reductions in plasma peptidoglycan. Consistent with the known modulatory effects of Firmicutes on bile acid (BA) metabolism, measurement of BAs demonstrated a significant increase of tauroursodeoxycholate (TUDCA), a neuroprotective BA, in *db/db* on IF but not in *db/db* on AL feeding. TGR5, the TUDCA receptor, was found in the retinal primary ganglion cells. Expression of TGR5 did not change with IF or diabetes. However, IF reduced retinal TNF-α mRNA, which is a downstream target of TGR5 activation. Pharmacological activation of TGR5 using INT-767 prevented DR in a second diabetic mouse model. These findings support the concept that IF prevents DR by restructuring the microbiota toward species producing TUDCA and subsequent retinal protection by TGR5 activation.

Diabetes-related blindness is a personal catastrophe for the individual and affects more than 4.2 million Americans (1). Although diabetic retinopathy (DR) is commonly

[1]Department of Pediatrics, Indiana University School of Medicine, Indianapolis, IN
[2]Department of Neurosurgery, The University of Texas Health Science Center at Houston, Houston, TX
[3]Department of Surgery, Indiana University School of Medicine, Indianapolis, IN
[4]Department of Ophthalmology and Visual Sciences, University of Alabama, Birmingham, AL
[5]Department of Genetics, The University of Texas MD Anderson Cancer Center, Houston, TX
[6]Department of Cellular and Integrative Physiology, Indiana University School of Medicine, Indianapolis, IN
[7]Department of Ophthalmology, Indiana University School of Medicine, Indianapolis, IN
[8]Department of Anesthesia, Indiana University School of Medicine, Indianapolis, IN
[9]Department of Chemistry, Vanderbilt University, Nashville, TN
[10]Second Genome, Inc., San Francisco, CA
[11]Northeastern University, Boston, MA
[12]Department of Radiation Oncology, University of California, Los Angeles, Los Angeles, CA
[13]Department of Medicine, University of Alberta, Edmonton, Alberta, Canada
[14]Department of Pharmaceutics, University of Florida, Gainesville, FL
[15]Intercept Pharmaceuticals, New York, NY
[16]Department of Biochemistry and Molecular & Cellular Biology, Georgetown University, Washington, DC
[17]Department of Medicine, Indiana University School of Medicine, Indianapolis, IN
[18]Department of Ophthalmology, University of Florida, Gainesville, FL
[19]Department of Physiology, Michigan State University, East Lansing, MI

Corresponding author: Maria B. Grant, mariagrant@uabmc.edu.

Received 7 February 2018 and accepted 18 April 2018.

This article contains Supplementary Data online at http://diabetes.diabetesjournals.org/lookup/suppl/doi:10.2337/db18-0158/-/DC1.

E.B. and Y.Y. contributed equally to the manuscript.

See accompanying article, p. 1745.

classified as a microvascular complication of diabetes, it is now recognized that changes in the neural cells of the retina occur early in the natural history of the disease and that these changes precede alterations in the microvasculature (2,3). Current therapies for DR, such as laser photocoagulation, injection of anti-VEGF antibodies, or vitreoretinal surgery (4), only treat late-stage disease and selectively target the microvascular component of the disease, whereas therapies for the early stages are limited to preventive strategies, such as lifestyle changes.

Chronic calorie restriction and intermittent fasting (IF) represent nonpharmacological strategies for prevention and treatment of diseases, such as diabetes, obesity, and aging. However, calorie restriction can lead to nutrient deficiencies and fatigue (5,6), low metabolic rate, and increased risk for subsequent obesity (7), infertility (5), suppression of immunity (8), and susceptibility to viral infections (9,10). IF prevents the adverse effects of calorie restriction as it restricts feeding to only a part of the day or to certain days per week. Thus, IF may be a more beneficial strategy compared with chronic calorie restriction as it combines the beneficial effects elicited by fasting physiology and a recovery period during the feeding phase that facilitates regeneration and promotes tissue repair (11).

Accumulating evidence indicates that the gut microbiota contribute to key physiological functions, such as energy metabolism, metabolic signaling, and regulation of integrity of the gut barrier (12–14). Individuals with chronic diseases such as diabetes exhibit altered bacterial composition (15), which likely not only influences glucose metabolism but also, we reasoned, may contribute to development of complications. Gut microbes have a symbiotic relationship with the host: they digest exogenous, indigestible foods generating secondary metabolites that can affect host physiology and metabolize endogenous substrates in the absence of food during prolonged fasting.

An example of endogenous metabolites being converted to beneficial secondary metabolites by the microbiome is the generation of secondary bile acids (BAs). Primary BAs generated by the liver are highly hydrophobic and can cause colitis; however, intestinal bacteria convert them to more hydrophilic, less toxic, secondary BAs that are potent agonists for nuclear receptors and have physiological functions. Using the *db/db* mouse and an IF (fasting every other day) regimen for 7 months, we showed that IF prevented development of DR and increased generation of a secondary BA and neuroprotective agent tauroursodeoxycholate (TUDCA). We further demonstrated the relevance of TUDCA by demonstrating localization of TGR5, the receptor that mediates TUDCA's effects in the retina. In addition, the pharmacological activation of TGR5 using INT-767 in a second diabetes model prevented development of DR.

RESEARCH DESIGN AND METHODS

IF Treatment of Diabetic Animals

Male B6.BKS(D)-Lepr^{db}/J (stock number: 000697) homozygous Lepr$^{db/db}$ were diabetic and heterozygous Lepr$^{db/m}$ mice were used as controls (denoted as *db/db* and *db/m* hereafter). All mice were obtained from The Jackson Laboratory (Bar Harbor, ME) and housed in the institutional animal care facilities at the University of Florida (IACUC #201106420) with strict 12 h:12 h light:dark cycle; all studies were repeated at Indiana University (IACUC #10604 and #11167). Blood glucose levels were tested every 2 weeks in *db/db* mice. Animals were considered diabetic and used in the IF experiment if the serum glucose level was above 250 mg/dL on two consecutive measurements. The animals were fed ad libitum (AL) before the IF was initiated at 4 months of age. The *db/m* and *db/db* mice were each divided in two subgroups, AL feeding (control) and IF, wherein the animals were fasted for 24 h every other day for 7 months, beginning at night (Fig. 1*A*). Glycated hemoglobin was measured using the A1CNow+ kit (Bayer HealthCare, Sunnyvale, CA) on the day prior to euthanasia.

INT-767 Treatment of Diabetic Animals

Eight-week-old male DBA/2J mice (stock number: 00671) were obtained from The Jackson Laboratory and maintained on a 12 h:12 h light:dark cycle. Mice were injected with streptozotocin (STZ) (Sigma-Aldrich, St. Louis, MO) intraperitoneally (40 mg/kg made freshly in 50 mmol/L sodium citrate buffer, pH 4.5 [vehicle]) for 5 consecutive days or with vehicle only. Blood glucose levels were measured 1 week after the last STZ injection, and mice with glucose levels >250 mg/dL on 2 separate days were considered diabetic. DBA/2J mice were fed with a Western diet (WD) (21% milk fat, 0.2% cholesterol, TD88137) obtained from Harlan-Teklad (Madison, WI) after diabetes onset in the STZ groups and were treated for 8 weeks with either WD or WD containing INT-767 (30 mg/kg bw/day) (Intercept Pharmaceuticals, New York, NY) (18).

Acellular Capillaries

The eyes were fixed in 2% formalin, and trypsin digest was performed for analysis of acellular capillaries as previously published (16).

Microbiome Analysis

Fecal samples (n = 180) were obtained by collection every 4 h for 48 h. Genomic DNA was isolated from ~0.1 g using the PowerSoil DNA Isolation Kit (MO Bio, Carlsbad, CA), according to manufacturer's protocol. DNA was sent to Second Genome, Inc. (San Francisco, CA) for 16S rRNA gene V4 sequencing with the MiSeq platform. The full report and statistical analysis from Second Genome is available upon request.

Colon Morphometric Analysis

Colon tissue was collected at termination of the experiment, fixed in 10% buffered formalin, and paraffin-embedded according to standard procedures at the Indiana University–Purdue University Indianapolis Pathology Core. Ten-micrometer sections were cut and stained by either hematoxylin and eosin or periodic acid Schiff for mucin.

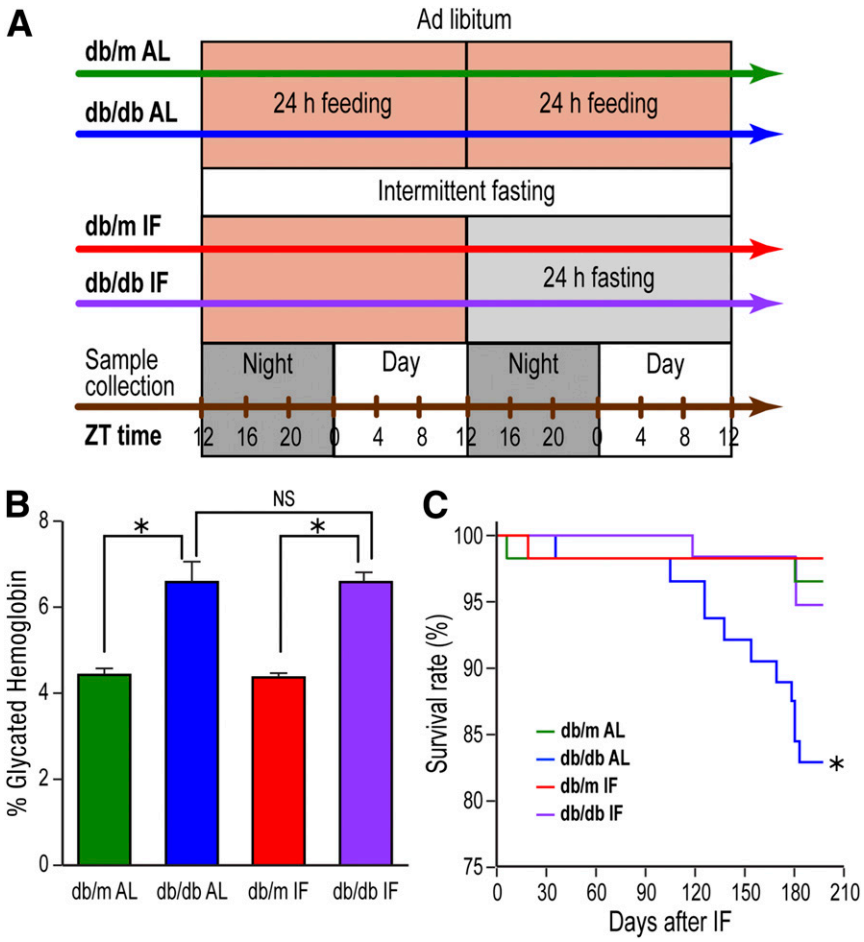

Figure 1—IF feeding prolonged survival of *db/db* mice without improving glycemic control. *A*: Depiction of the experimental protocol with the treatment groups. Mice were put on IF diet at 4 months of age and were held on IF for 7 months. ZT represents zeitgeber time, i.e., time when the lights went on. *B*: Glycated hemoglobin levels in *db/db*-AL and *db/db*-IF mice were higher compared with *db/m* mice; however, IF did not correct glycated hemoglobin levels. Data represent means ± SEM (n = 6–39). *$P < 0.05$. *C*: *db/db*-AL had reduced survival compared with *db/m* mice. IF improved survival rate of *db/db*-IF mice compared with that of normal controls. *$P < 0.05$.

Entire sections were scanned with an Axio Scan Z1 (Zeiss) and a 20× objective. Morphometric analysis of goblet cells, villi length, and muscularis thickness was undertaken using a Lumenera Infinity 1-2C camera and NIS Elements software (Nikon Instruments, Melville, NY).

Peptidoglycan ELISA

Plasma samples were diluted 1:10 and analyzed for peptidoglycan levels using the mouse peptidoglycan ELISA kit (MBS263268; Mybioscource Inc., San Diego, CA), according to manufacturer's instructions.

BA Analysis

At the termination of the experiment, whole blood was collected by cardiac puncture and transferred in EDTA-coated tubes. Plasma was separated and frozen at −80°C. Samples were sent to Metabolon Inc. (Morrisville, NC), and global metabolic analysis was performed with their Metabolon Platform using a Waters ACQUITY ultra-performance liquid chromatography and a Thermo Scientific Q-Exactive high resolution/accurate mass spectrometer interfaced with a heated electrospray ionization source and Orbitrap mass analyzer operated at 35,000 mass resolution. The full report and statistical analysis from Metabolon is available upon request.

Quantitative Real-time PCR

Total RNA was extracted from mouse retinal tissue using RNeasy Mini kit (Qiagen, Germantown, MD), and reverse transcription was performed, according previous published methods (17). Validated primers for *Gpbar1* (TGR5), *Tnf*, and endogenous controls *B2m* and *Ppia* were purchased from Qiagen, and quantitative real-time PCR was carried out using SYBR Green (Qiagen).

Immunofluorescence Staining

Enucleated eyes were fixed in 4% paraformaldehyde overnight at 4°C. The next day, eyes were incubated with 30% sucrose for 48 h and then quickly frozen in optical cutting temperature compound. Retinal cross-sections (12 μm) were cut at −20°C. The following antibodies were used for immunostaining: rabbit monoclonal to IBA-1 (019–19741, Wako; 1:500), rat monoclonal to CD45 (clone

30-F11, R&D Systems; 1:50), rabbit polyclonal to GPCR TGR5 (ab72608, Abcam; 1:250), and monoclonal murine anti-NeuN (clone A60, MAB377MI, EMD Millipore; 1:250). Sections were preincubated with 5% goat serum (Invitrogen) in PBS for 1 h, followed by incubation with primary antibodies (in 1% normal goat serum) overnight at 4°C. As a secondary antibody, Alexa Fluor 488 was used for TGR5 and IBA-1, and Alexa Fluor 594 was used for NeuN and CD45 (Invitrogen). Positive cells were counted from 3 to 5 sections at 100-μm intervals for each eye, on at least four images per section at 20× magnification. Retinal sections were imaged using a confocal scanning laser microscope (ZEISS LSM 700 confocal microscope system with Axio Observer; Carl Zeiss Mditec, Jena, Germany), and colocalization was analyzed by using ZEN lite software.

Statistical Analysis

Survival curve was plotted by Kaplan-Meier method, and the significance of the differences was determined by log-rank test. The differences in gene expression, metabolites, and acellular capillaries were analyzed by two-way ANOVA followed by Tukey honest significant difference post hoc test (GraphPad Prism, La Jolla, CA). Statistical analysis methods for microbiome and metabolites are available upon request.

RESULTS

IF Improved Survival Without Impacting Glycated Hemoglobin Levels

Four-month-old *db/m* and *db/db* mice were fed either an AL diet or were fasted on an every other 24-h interval (IF) for 7 months (Fig. 1*A*). Glycated hemoglobin levels were not affected by the IF regimen and remained higher in both *db/db* cohorts compared with controls (Fig. 1*B*). However, despite no change in glycated hemoglobin, the survival rate increased significantly in *db/db* mice on the IF regimen (*db/db*-IF) compared with *db/db* mice on AL feeding (*db/db*-AL) (Fig. 1*C*).

IF Prevented Development of Acellular Capillaries and Infiltration of Inflammatory Cells in the Retina of *db/db* Mice

We next examined the impact of IF on the development of DR in *db/db* mice by enumerating acellular capillaries (Fig. 2*A–D*) (19). As expected, *db/db*-AL mice showed increased numbers of acellular capillaries (Fig. 2*C*) compared with age-matched *db/m*-AL mice (Fig. 2*A*). However, *db/db*-IF mice (Fig. 2*D* and *E*) did not demonstrate an increase in acellular capillaries. As increases in retinal levels of inflammatory cells are another feature of DR, cryosections were examined for changes in activated microglia using IBA-1 staining and differences in infiltrating hematopoietic cells using CD45 staining. *db/db*-AL mice showed a significant increase in IBA-1$^+$ cells compared with *db/m*-AL mice and *db/db*-IF mice (Fig. 2*F*). CD45$^+$ cell infiltration was significantly increased in the *db/db*-AL mice compared with the *db/m*-AL mice and *db/db*-IF mice (Fig. 2*G*). Overall, IF protected *db/db* mice from developing histological features of DR.

Long-term IF Altered the Gut Microbiome Composition

The composition and diversity of the microbiome is integrated with the pathophysiology of diabetes. For example, certain bacteria are shown to induce diabetes (20), whereas others alleviate it (21). Thus, we hypothesized that the beneficial effects of IF on DR would, at least in part, be mediated through changes in microbiota composition. Fecal samples were collected and genomic DNA sequencing was used to discover and distinguish various bacterial taxa. A total of 1,363 filtered operational taxonomic units (OTUs) were detected. Sample richness and Shannon diversity (Supplementary Fig. 1*A–F*) were not changed by the implementation of IF but β diversity, a measure of the between-sample diversity, showed clear differences between *db/db*-AL and *db/m*-AL (Fig. 3*A*), *db/m*-IF vs. *db/m*-AL (Fig. 3*B*), and *db/db*-IF vs. *db/db*-AL (Fig. 3*C*) mice. Principal component analysis of bacteria also demonstrated a clear separation of the four main groups (*db/m* AL, *db/db* AL, *db/m* IF, and *db/db* IF). The AL groups were closer to each other, whereas the IF groups diverged more (Fig. 3*D*). This evidence suggests that IF restructured a distinct microbiome in diabetic compared with control mice.

The most represented phyla were Bacteroidetes, Firmicutes, Verrucomicrobia, Tenericutes, Actinobacteria, and Proteobacteria. The relative proportions of these varied dramatically among the experimental groups but the majority of bacteria belonged to the Bacteroidetes, Firmicutes, and Verrucomicrobia phyla (Fig. 3*E*). The ratio of Firmicutes/Bacteroidetes (F/B) has been widely used as an indicator of changes in the microbiome with obesity (22). The F/B ratio was not altered in the *db/m*-IF mice (Fig. 3*E*); however, it was dramatically increased in the *db/db*-IF mice due to a significant increase of Firmicutes and a significant reduction of Bacteroidetes (Fig. 3*E*). Apart from changes observed in the F/B ratio, Verrucomicrobia also changed significantly with IF showing an increase in *db/m*-IF and a reduction in *db/db*-IF mice (Fig. 3*E*). Overall, these data indicate that IF resulted in a more dramatic restructuring of the microbiota composition in diabetic mice, with a significant expansion of Firmicutes at the expense of Bacteroidetes and Verrucomicrobia.

To understand how the microbiota composition was altered at the genus level, the differential taxa in each group were assessed (Fig. 4*A–C*). Among the differential taxa between *db/m*-AL and *db/db*-AL cohorts, the *db/db*-AL mice were enriched in *Lactobacillus*, *Bifidobacterium*, *Bacteroides*, and *Akkermansia* and were deficit in species of *Oscillospira* and *Ruminococcus* (Fig. 4*A*). The IF regimen in the *db/db* mice caused enrichment of species of the genus *Lactobacillus*, *Oscillospira*, and *Ruminococcus* and reduction of species of the genus *Akkermansia*, *Bacteroides*, and *Bifidobacterium* (Fig. 4*B* and *C*). Interestingly, the difference in the microbiota between fed and fasting state in the

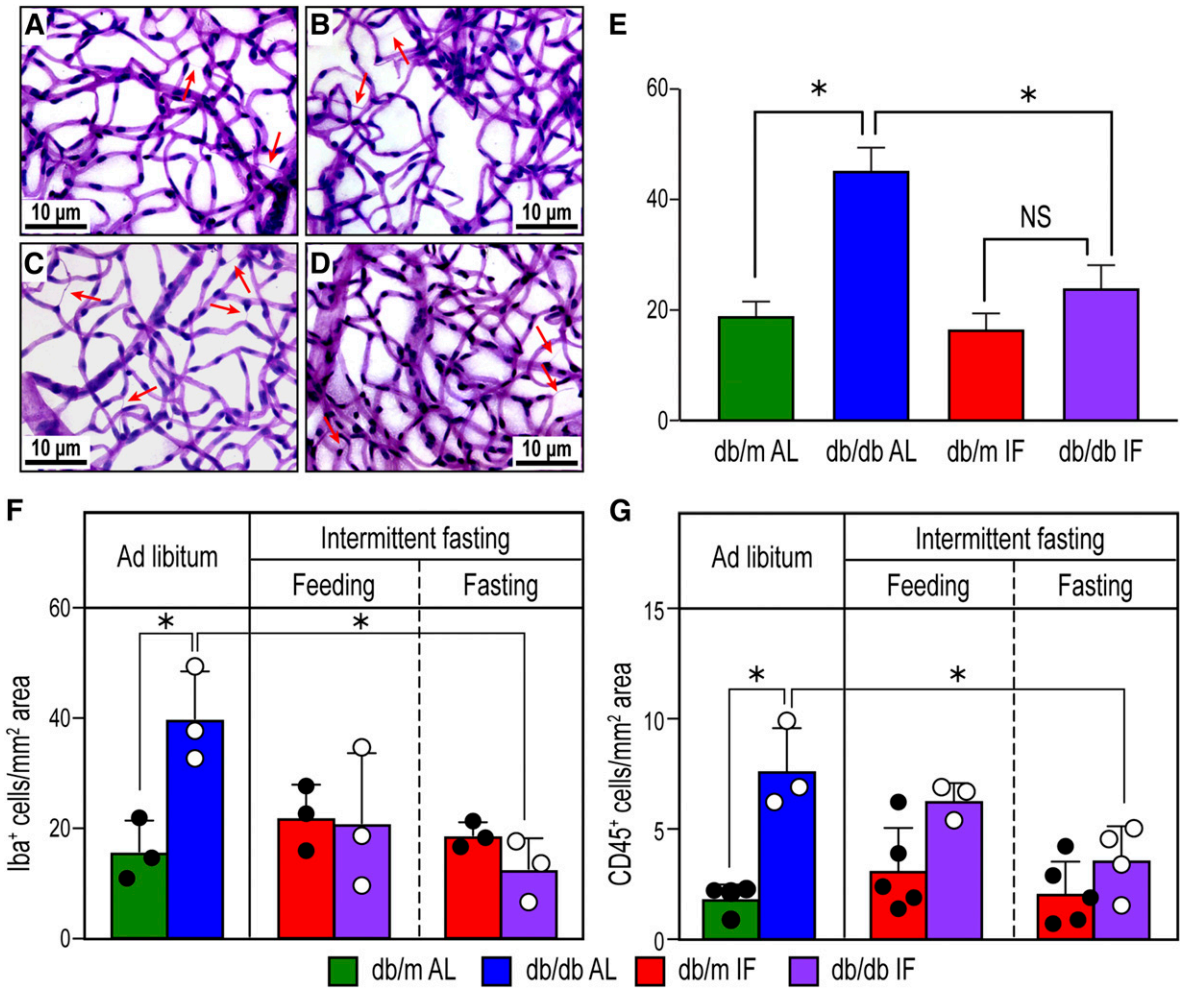

Figure 2—IF reduced DR in *db/db* mice. *A–D*: Representative images of the trypsin-digested retinas from the four experimental groups: *db/m* AL (*A*), *db/m* IF (*B*), *db/db* AL (*C*), and *db/db* IF (*D*). Arrows indicate acellular capillaries. Scale bars: 10 μm. *E*: Enumeration of acellular capillaries per mm^2 retinal area. Data represent means ± SEM ($n = 10$). *$P < 0.05$, one-way ANOVA. *F*: Enumeration of IBA-1$^+$ cells per mm^2 retinal area from immunofluorescence-stained retina cryosections. Data represent means ± SEM ($n = 3$). *G*: Enumeration of CD45$^+$ cells per mm^2 retinal area from immunofluorescence-stained retina cryosections. Data represent means ± SEM ($n = 3$–5). *F* and *G*: *$P < 0.05$, two-way ANOVA.

IF cohorts was very small, limited to only 24 bacteria in *db/db*-IF mice and 69 bacteria in *db/m*-IF mice (Supplementary Fig. 2*A* and *B*). Yet, we identified certain common species that were increased by fasting in both *db/m*-IF and *db/db*-IF cohorts, mostly species in the Lachnospiraceae and Ruminococcaceae families with representatives from *Oscillospira* and *Ruminococcus* genera. On the other hand, species of the genus *Bifidobacterium* were commonly reduced by the IF diet. A list of the common and unique enriched bacterial species is shown in Supplementary Fig. 2*C* and the common or uniquely reduced bacteria is shown in Supplementary Fig. 2*D*.

IF is known to influence diurnal rhythms and selected microbes in the gut exhibit diurnal changes (23,24). We investigated which taxa displayed diurnal patterns in healthy *db/m*-AL mice and whether these taxa were affected by either the presence of diabetes or IF (25). Surprisingly, we found only 34 OTUs showing diurnal cycling. Among these were members of Lachnospiraceae and Ruminococcaceae families, specifically species of *Oscillospira* and *Ruminococcus*. Examples of bacteria with diurnal regulation are shown in Supplementary Fig. 3.

Although there were few taxa differentially regulated by feeding/fasting or diurnal cycling, the evolutionary pressure of fasting and refeeding in combination with the host metabolic response to fasting led to the distinct restructuring of the microbiota in the *db/m*-IF and *db/db*-IF mice. Members of the order Clostridiales (Fig. 4*D*) and members of the *Ruminococcaceae* (Fig. 4*E*) and *Lachnospiraceae* families (Fig. 4*F*) were uniquely equipped to adapt, expand, and survive under IF conditions in *db/db* but not in *db/m* mice. Lactobacillus (Fig. 4*G*) was enriched in both *db/m*-IF and *db/db*-IF mice, whereas the genera *Bifidobacterium* (Fig. 4*H*) and *Clostridium* (Fig. 4*I*) were reduced in both groups. On the other hand, *Oscillospira* (Fig. 4*J*), *Ruminococcus* (Fig. 4*K*), and *Turicibacter* (Fig. 4*L*) were enriched

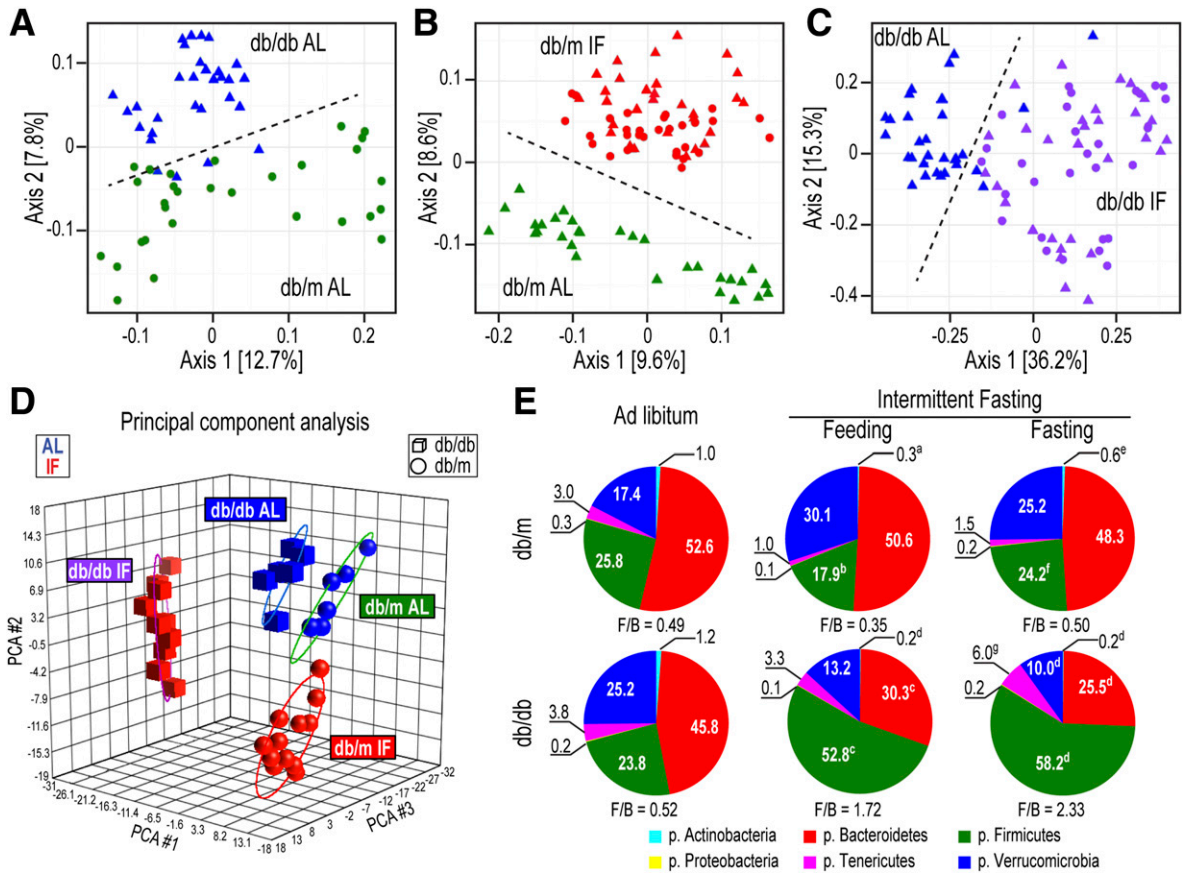

Figure 3—IF resulted in distinct changes in the microbiota of *db/db* mice. *A–C*: β Diversity (presence/absence ordination): Dimensional reduction of the Jaccard distance on presence/absence OTU table, using the PCoA ordination method. *A*: *db/m*-AL (green circles) vs. *db/db*-AL (blue triangles) mice; samples separated along axis 2 according to sample type. *B*: *db/m*-AL (green triangles) vs. *db/m*-IF (feeding, red triangles; fasting, red circles) mice; samples separated along axis 2 according to type, which indicated that samples from IF and AL treatments have different incidences of OTUs. *C*: *db/db*-AL (blue triangles) vs. *db/db*-IF (feeding, purple triangles; fasting, purple circles) mice; samples separated along axis 1 according to type. Samples from *db/db*-AL mice had a smaller degree of variation in microbiome β diversity than *db/db*-IF samples. $P = 0.001$ in all comparisons; $n = 5$ mice/group. *D*: Principal component analysis (PCA) of microbiota. Relative abundance of bacteria present in at least 10% of the samples ($n = 180$) was used. Samples grouped by both disease (spheres, *db/m*; cubes, *db/db*) and treatment (blue, AL; red, IF) but less clearly by feeding/fasting within the IF groups. Note that the AL cohorts are closer to each other, whereas the IF cohorts were much further apart, suggesting bigger differences in the microbiomes of *db/m*-IF and *db/db*-IF mice. *E*: Relative proportions of the six most abundant phyla (the aggregate relative abundance for each of the phyla not represented here is less than 0.1). $^{a}P < 0.01$ vs. *db/m*-AL; $^{b}P < 0.001$ vs. *db/m*-AL; $^{c}P < 0.05$ vs. *db/db*-AL; $^{d}P < 0.001$ vs. *db/db*-AL; $^{e}P < 0.05$ vs. *db/m* IF (feeding); $^{f}P < 0.001$ vs. *db/m* IF (feeding); $^{g}P < 0.05$ vs. *db/db* IF (fasting). All OTUs (detected in at least 10% of the samples) from all samples per each group were used, irrespective of zeitgeber time. p., phylum.

specifically in the *db/db*-IF mice, whereas *Bacteroides* (Fig. 4*M*), *Akkermansia* (Fig. 4*N*), and *Allobaculum* (Fig. 4*O*) were reduced only in the *db/db*-IF mice. We reasoned that these unique changes in the microflora of the *db/db*-IF mice could promote the integrity of the gut barrier.

IF Promoted Restoration of Diabetes-Induced Gut Pathology

As disruption of the gut barrier integrity is an important mechanism of disease, we examined whether IF beneficially impacted colon morphology as measured by goblet cell number and villi length (Fig. 5). *db/db*-AL mice had reduced numbers of goblet cells (Fig. 5*B* and *E*) and reduced villi length (Fig. 5*G* and *J*). However, IF resulted in preservation of colon morphology in the *db/db*-IF mice, as goblet cell number (Fig. 5*D* and *E*) and villi length (Fig. 5*I* and *J*) were similar to nondiabetic mice. No changes with diabetes or IF were observed in the thickness of the muscularis (Fig. 5*K–O*).

Increases in bacterial products in plasma are indicative of intestinal barrier dysfunction or disruption. We measured peptidoglycan in plasma samples from our cohorts. As shown in Fig. 5*P*, *db/db*-AL demonstrated a significant increase in plasma peptidoglycan levels supportive of increased gut permeability. IF resulted in a decrease in gut permeability when *db/db*-IF mice were in the fasted state as there was a significant reduction of circulating peptidoglycan levels. However, when the *db/db*-IF mice were in the fed state this potentially beneficial change was lost.

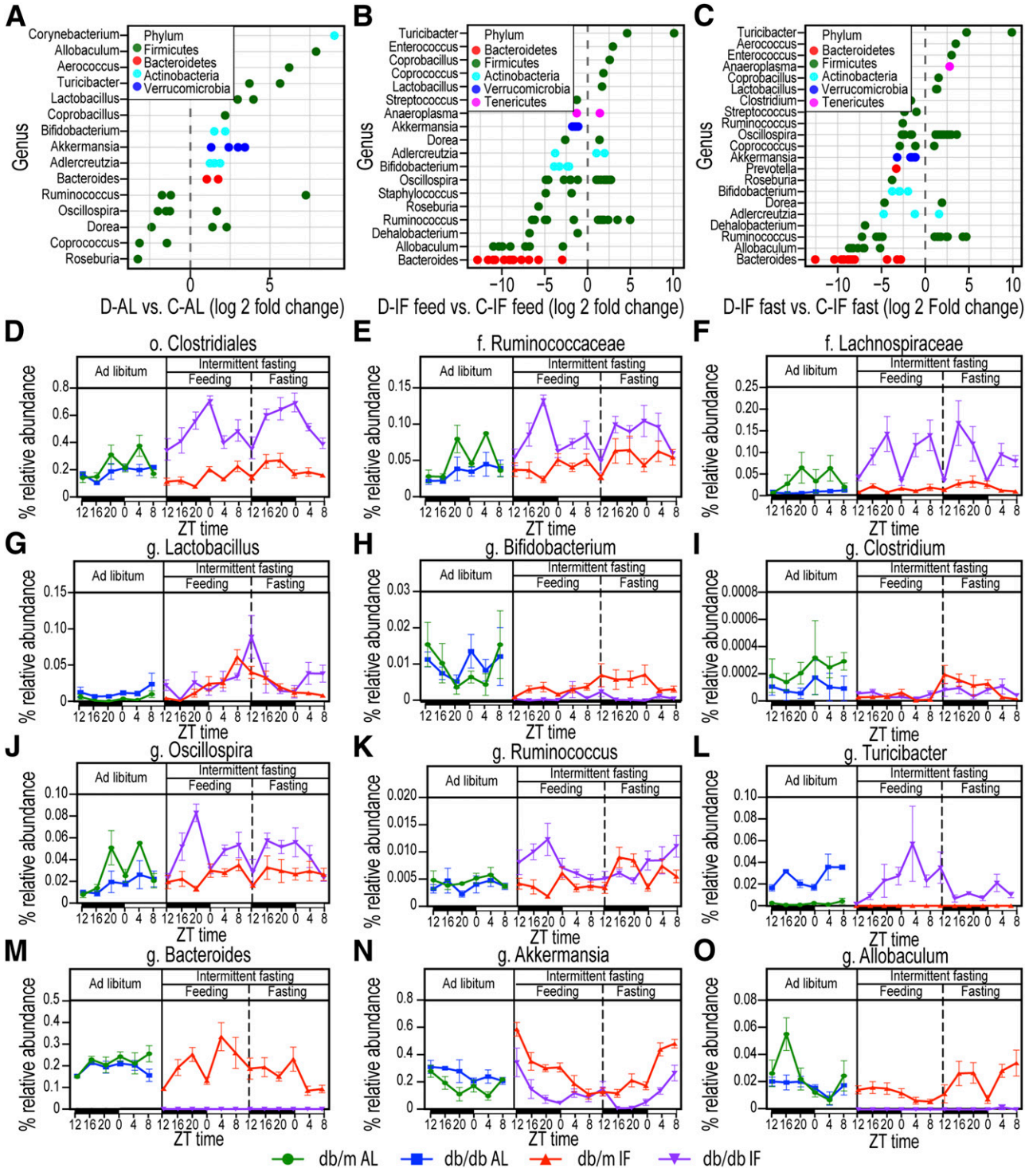

Figure 4—IF effects on microbiome composition at the genus level. *A*: Genera that show statistically significant changes in *db/db*-AL vs. *db/m*-AL mice. *B*: Genera that were statistically different in *db/db*-IF vs. *db/m*-IF mice in the feeding phase. *C*: Genera that were statistically different in *db/db*-IF vs. *db/m*-IF in the fasting phase. Points are OTUs belonging to each respective genus. Features were considered significant if false discovery rate–corrected *P* value ≤0.05 and the absolute value of $\log_2$ fold change ≥1. *D–O*: Time course of relative bacterial abundances of selected taxa during the 48-h cycle of IF regimen are shown. ZT represents zeitgeber time, i.e., time when the lights went on. Diurnal oscillations in selected taxa and IF effects: o. Clostridiales (*D*), f. *Ruminococcaceae* (*E*), f. *Lachnospiraceae* (*F*), g. *Lactobacillus* (*G*), g. *Bifidobacterium* (*H*), g. *Clostridium* (*I*), g. *Oscillospira* (*J*), g. *Ruminoccocus* (*K*), g. *Turicibacter* (*L*), g. *Bacteroides* (*M*), g. *Akkermansia* (*N*), and g. *Allobaculum* (*O*). Data are sums of relative abundance of all OTUs within each genus ± SEM. f., family; g., genus; o., order.

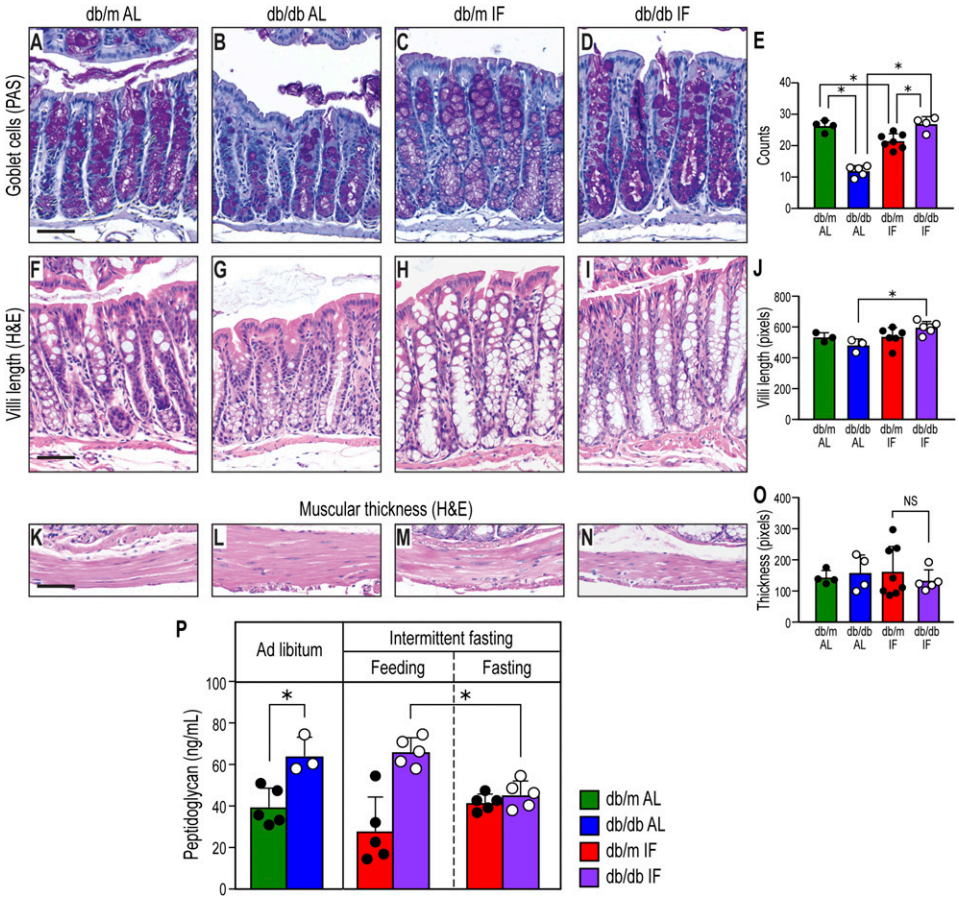

Figure 5—IF treatment affected gut morphology. *A–D*: Periodic acid Schiff (PAS) staining showing mucin-positive goblet cells. Diabetes reduced goblet cell number, but IF prevented this reduction. *E*: Quantification of goblet-positive cells. Data represent number of goblet cells/villus. *$P < 0.05$, n = 13–30 villi/group. *F–I*: Hematoxylin and eosin (H&E) staining of colon. The length of villi was reduced significantly with diabetes, but IF restored levels to normal. *J*: Quantification of the villi length, in pixels. *$P < 0.05$, n = 17–26 villi/group. *K–N*: Hematoxylin and eosin staining of the muscularis layer. *O*: Quantification of the muscularis width. Twenty measurements distributed evenly were done on each section, and data represent averages per section in pixels ± SD; n = 4–7 sections/group. In all cases, one section per mouse was analyzed. Scale bars: 50 μm. *P*: Peptidoglycan, a component of bacterial cell wall, was measured in plasma from the cohorts using ELISA. Data represent means ± SD (n = 3–5). *$P < 0.05$, two-way ANOVA.

IF Altered BA Metabolism

We next tested whether the microbial changes induced by IF could generate beneficial metabolites. BAs are known to alter the gut microbiome composition (26), and conversely, the microbiome is known to alter the BA pool (27). Thus, we reasoned that the observed microbiome changes induced by IF would impact BA metabolism in the *db/db* mice. Metabolic analysis of plasma from the experimental cohorts identified the primary BA cholate but not chenodeoxycholate. A list of BAs found in the plasma is shown in Supplementary Table 1.

Cholate was increased in the *db/db*-AL mice compared with *db/m*-AL mice and was reduced in the *db/db*-IF mice (Fig. 6*A*). Deoxycholate, the secondary BA that is produced by the activities of 7α-dehydroxylase, an enzyme found in intestinal bacteria, was moderately increased with IF especially during the fasting period (Fig. 6*B*), supporting intestinal transformation of BAs. However, the ratio of conjugated to unconjugated BA was increased in the *db/db*-IF compared with *db/m*-IF mice during feeding, suggesting that there may be a reduction of bacteria that express bile salt hydrolase activity required to deconjugate primary and secondary BAs in the *db/db*-IF mice. A significant reduction of *Bifidobacterium* (Fig. 4*H*), *Clostridium* (Fig. 4*I*), and *Bacteroides* (Fig. 4*M*) was observed, and these bacteria are known to express bile salt hydrolase, which may be responsible, in part, for these observed changes in levels of conjugated to unconjugated secondary BAs.

An increase in BA products indicative of 7α- and 7β-hydroxysteroid dehydrogenase (HSDH) enzymatic activity was also found. Taurochenodeoxycholate (TCDCA) was identified and significantly increased in the *db/db*-IF mice (Fig. 6*C*). TCDCA is converted to TUDCA by the actions of both 7α- and 7β-HSDH (28), and TUDCA was significantly increased in the plasma of *db/db*-IF mice (Fig. 6*D*). As taurine-conjugated secondary BAs are potent activators of TGR5 (29), we hypothesize that the beneficial effects we observed following IF were due to an increase in TUDCA synthesis in the gut.

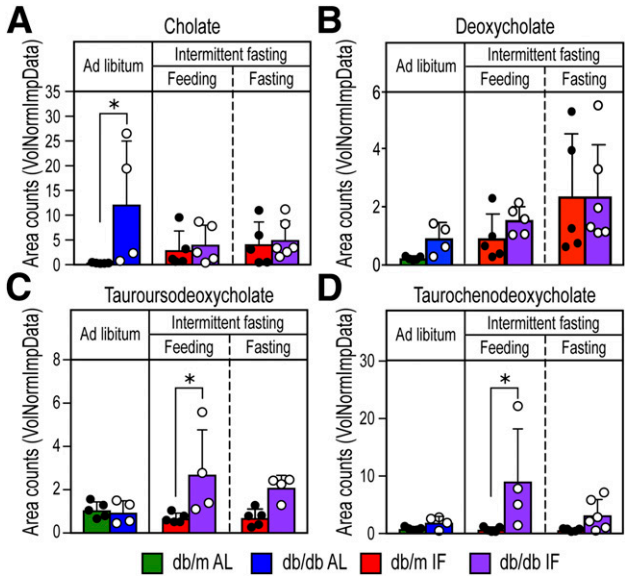

Figure 6—IF enhanced BA metabolism with increases in the neuroprotective BA TUCDA. Analysis of plasma samples for BA metabolites cholate (*A*), deoxycholate (*B*), TUDCA (*C*), and TCDCA (*D*). TCDCA and TUDCA were significantly increased with IF diet in the db/db-IF mice. TCDCA is converted to TUDCA by the actions of both 7α- and 7β-HSDH. Values for each sample are normalized by sample volume/utilized for extraction. Each biochemical is then scaled to set the median equal to 1. Missing values are imputed with the minimum. Data represent means ± SD (n = 4–6). *$P < 0.05$, two-way ANOVA.

TGR5 Activation Reduces Acellular Capillaries and Inflammation in the Diabetic Retina

To determine whether TUDCA could mediate beneficial effects in the retina, we examined TGR5 expression. TGR5 was localized primarily to the ganglion cell layer of the retina (Fig. 7*A*). Neither diabetes nor the IF regimen changed the localization or expression of TGR5 protein (Fig. 7*B–F*), as assessed by immunohistochemistry, or changed TGR5 mRNA levels (Fig. 7*G*). However, TNF-α, a downstream target of TGR5, was reduced significantly by IF in the diabetic cohort (Fig. 7*H*). To further support the role of retinal TGR5, we asked if pharmacological activation of TGR5 would prevent DR. Previously, we characterized the novel highly potent semisynthetic BA derivative and dual TGR5/FXR agonist INT-767 (18). INT-767 was tested in a second diabetes model, DBA/2J mice treated with STZ and placed on a high-fat diet. This model exhibits a more rapid progression of the vascular and inflammatory end points associated with DR (30) and diabetic nephropathy (31) and replicates the natural history and metabolic characteristics of human metabolic syndrome and type 2 diabetes (31,32). INT-767 treatment of diabetic mice resulted in a marked reduction in the number of acellular capillaries (Fig. 7*I*) and reduced numbers of $CD11b^+$ macrophages (Fig. 7*K*), $CD45^+$ leukocytes (Fig. 7*J*), and activated $IBA\text{-}1^+$ microglia within the retina (Fig. 7*L*).

DISCUSSION

The salient findings of this study suggest that restructuring of the microbiome by IF favors generation of secondary BAs, such as TUDCA, eliciting protective effects in the retina (Fig. 8). Development of acellular capillaries, activation of retinal microglia, and infiltration of peripheral immune cells into the retina were all reduced by IF in the *db/db* mice. IF produced a reconfiguration of the microbiota in the *db/db* mice resulting in an enrichment in Firmicutes and a reduction in Bacteroidetes. Interestingly, this was not observed for *db/m* mice undergoing IF, indicating that the diabetic microenvironment benefited Firmicutes expansion. High F/B ratio has been associated with healthy obesity (33,34) and increased capacity for harvesting energy (22). In addition, a high F/B ratio has been implicated in regulating fat storage (35) and is consistent with our findings wherein IF did not change the weight of the *db/db* mice but promoted a healthier obese phenotype with increased longevity.

Another example of a healthy obese phenotype associated with expansion of Firmicutes is the case of black bears. During the summer when active and feeding, these bears experience a healthy weight gain and an expansion of Firmicutes (36). Our study provides support for the clinical observation that some obese individuals are metabolically healthy (ranging from 3 to 57%, depending on the study) (13) and may have a gut microbiota structure that contributes to this beneficial outcome.

BAs are significant modulators of the gut microbiome as they exhibit antimicrobial activities and can inhibit bacteria outgrowth (37). Members of the Firmicutes phylum are expanded in high BA conditions, whereas members of Bacteroidetes and Actinobacteria (*Bifidobacterium*) are reduced (26). This finding is particularly relevant, as it appears that the *db/db*-AL mice have increased cholate compared with *db/m*-AL mice. The altered BA metabolism observed in the diabetic mouse effectively drove the restructuring of the diabetic microbiota toward the unique composition with high F/B ratio.

The observed changes in the gut microbiome of *db/db*-IF mice were deemed advantageous for gut and intestinal barrier integrity. We used plasma peptidoglycan as a surrogate for gut barrier function. Peptidoglycan levels were increased in diabetes, and the IF diet reduced the levels during fasting. This suggests that gut barrier integrity is compromised by diabetes and that the IF regimen (during the fasting day) can improve it. Our results are in agreement with a recent study demonstrating that hyperglycemia drives the increased intestinal permeability observed in diabetes (38). In our model, when diabetic mice are under IF, glucose remains elevated during the feeding day of the IF regimen but is reduced during the fasting phase of the IF regimen. Furthermore, the composition of the leaked bacteria may be important in driving the low-grade systemic inflammation in diabetes (39). Peptidoglycan is a component of gram-positive bacteria, and endotoxin is mostly derived from gram-negative bacteria. Firmicutes are gram positive, and *Bacteroides* are gram negative (40). Thus, our results suggest that the reduction of peptidoglycan occurring in the *db/db* mouse on the IF regimen signals a transient

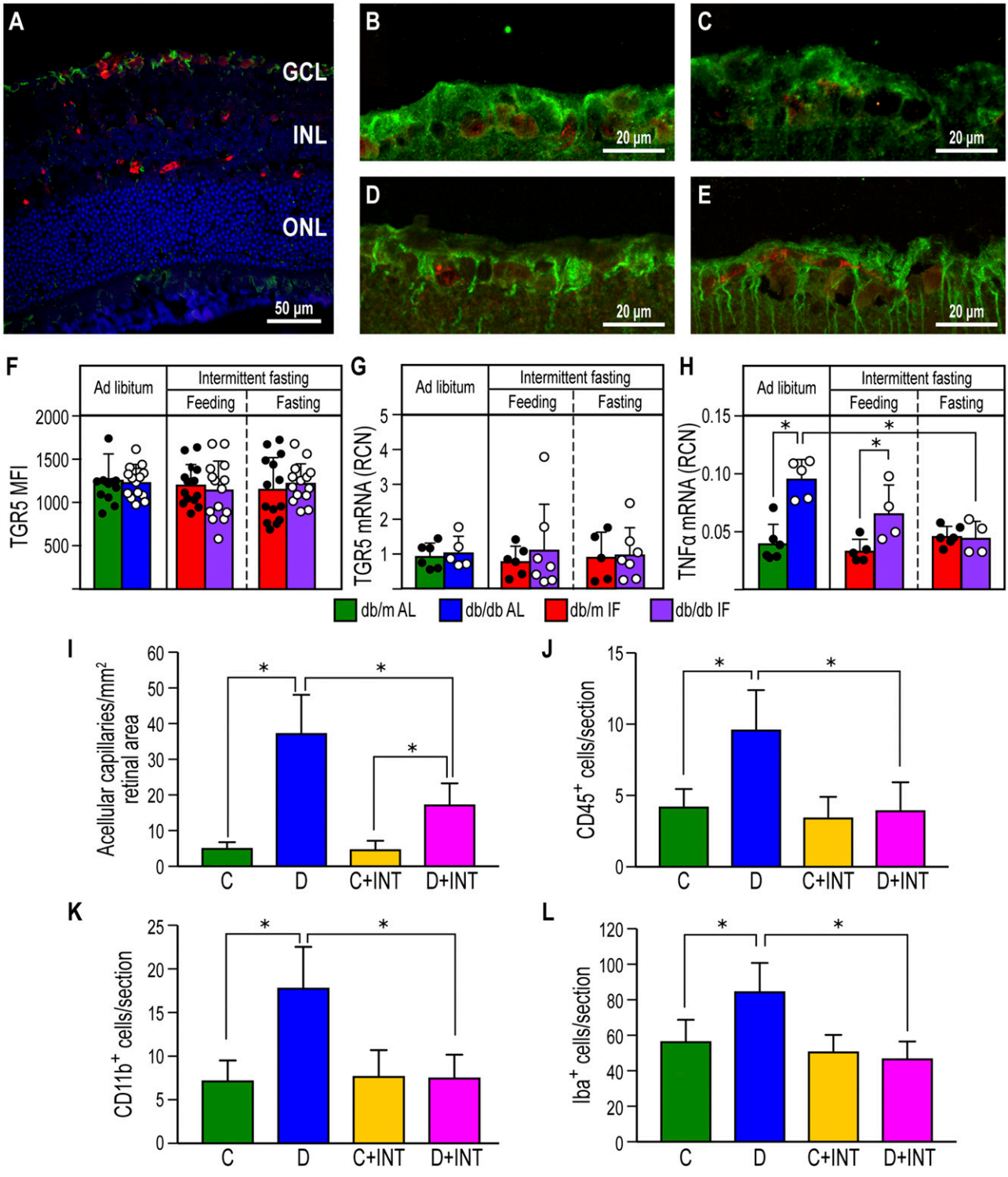

Figure 7—TGR5 activation using the BA agonist INT-767 prevented DR. *A*: TGR5 immunofluorescence staining is located in the retinal ganglion cell layer of a *db/m* control mouse. NeuN is used as a marker of ganglion cells. TGR5: green, NeuN: red, and DAPI: blue. INL, inner nuclear layer; GCL, ganglion cell layer; ONL, outer nuclear layer. *B–E*: TGR5 and NeuN staining in *db/m*-AL (*B*), *db/m*-IF (*C*), *db/db*-AL (*D*), and *db/db*-IF (*E*). *F*: Quantification of the fluorescence intensity of TGR5 in the retinal ganglion cell layer. Data represent means ± SD (n = 10–12). *G*: TGR5 mRNA expression in retinas from all cohorts. Data represent means ± SD (n = 5–7). *H*: TNF-α mRNA expression in retinas from all cohorts. Data represent means ± SD (n = 4–5). *$P < 0.05$, two-way ANOVA. *I–L*: Effects of INT-767 on retinas of 20-week STZ-diabetic DBA/2J mice. *I*: INT-767 protects from development of DR as measured by enumeration of acellular capillaries. *J*: INT-767 returns $CD45^+$ cell numbers to levels seen in no diabetic mice. *K*: Inflammatory monocytes are reduced in the INT-767–treated mice, as shown by quantification of $CD11b^+$ cells. *L*: INT-767 reduced numbers of IBA-1^+ cells within the retina. C, DBA/2J mice fed with vehicle; C+INT, DBA/2J mice fed with INT-767; D, STZ/WD mice; D+INT, STZ/WD with INT-767. Data represent means ± SD (n = 6 per group). *$P < 0.05$, one-way ANOVA.

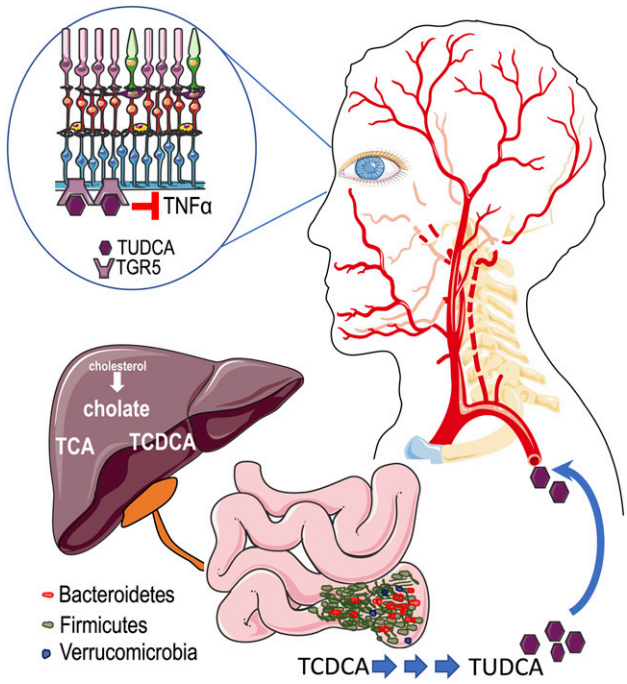

Figure 8—A model for IF-induced changes in the microbiome and their potential impact on development of DR. In diabetic mice, IF resulted in significant expansion of bacteria of the Firmicutes phylum that metabolize primary BAs to secondary BAs, such as TUDCA. TUDCA then enters the circulation and crosses the blood-retina barrier, targets its receptor, TGR5, in the ganglion cell layer and protects against retinal neurodegeneration and inflammation.

restoration/improvement in gut integrity and could also lead to a transient reduction in endotoxemia. However, this remains to be tested.

In diabetes, cholesterol and BA metabolism is altered (41). Thus, we focused our efforts in understanding how remodeling of the microbiota by IF affected biotransformation of the BA pool. Primary BAs are synthesized from cholesterol in the liver and act as detergents for the emulsification of dietary fats and as endocrine hormones for the regulation of glucose and lipid metabolism (42,43). Conjugated or unconjugated primary BAs enter the gallbladder and are released in the small intestine, where BA are structurally modified into various secondary BAs that are less toxic to the host and can exert multiple hormonal regulatory roles (44). 7α-HSDH and 7β-HSDH are two key enzymes that drive the efficient biosynthesis of secondary BAs such as TUDCA from TCDCA (28). Thus, the change in microbiome composition affects the enzymatic activity of these pathways and alters the BA pool.

Of interest is the observation that bear bile has long been used in Chinese traditional medicine for the treatment of liver, gallbladder, heart, and eye problems. Bear bile is highly enriched in TUDCA (45). Recently, the bear gut microbiome was used to isolate new, undiscovered 7β-HSDH enzymes for more efficient production of TUDCA (28). Little is known regarding the protective effects of TUDCA in the diabetic retina (46–52). However, this hydrophilic BA can cross the blood-brain barrier and likely can cross the blood-retinal barrier. In support of the ability of circulating TUDCA to reach the retina and act on retinal cells are the observations that TUDCA can inhibit photoreceptor apoptosis (47,48,51), improve retinal pigment epithelial function (49), inhibit proliferation of human retinal endothelial cells (53), promote the recruitment of endothelial progenitor cells (54), and protect against DR (53). At the molecular level, TUDCA has been shown to inhibit apoptosis through reduction of endoplasmic reticulum stress (55) and modulation of the unfolded protein response (56). TUDCA also inhibits mitochondrial membrane depolarization (57). Receptor activation of TGR5 by TUDCA may also decrease the production of proinflammatory cytokines and induce anti-inflammatory responses (58). Although TGR5 protein expression did not change with IF treatment, our studies would support that TGR5 activation is central to the retinal protection observed, possibly through eliciting anti-inflammatory effects, as INT-767 effectively prevented DR and reduced infiltration of inflammatory cells in the retina of STZ-treated DBA/2J mice fed a WD that included vehicle (STZ/WD). Although INT-767 is known as a dual agonist of TGR5 and FXR, the absence of FXR in the retina (59) allowed us to use this highly potent agent as a selective TGR5 agonist in the retina. However, additional studies will be required to establish a direct link between TGR5 activation and IF.

Our study has certain limitations that must be acknowledged. First, fecal rather than mucosal bacterial samples were used. As such, our analysis may not be representative of the entire microbiome. However, fecal sampling is typically used in human studies. Second, we used plasma samples rather than cecum samples for the analysis of metabolites. Our intention was to identify microbial metabolites that could be found in peripheral circulation, specifically those that could target the retina. Third, we used the *db/db* model as a model of type 2 diabetes to study the IF effects on microbiota. The STZ/WD model of diabetes was used to establish the link between TGR5 activation and prevention of DR. The STZ/WD represents an accelerated model of DR that histologically replicates DR seen in other diabetes models (30) and also has the natural history and metabolic characteristics of human metabolic syndrome and type 2 diabetes (31,32). Finally, although we show an association between increases in TUDCA and prevention of retinopathy, additional studies using antibiotics or fecal transfers will be required to demonstrate this conclusively.

In sum, our study shows a novel relationship between changes in the microbiota, IF, and increases in TUDCA. IF likely provides a way to change BA metabolism in favor of increasing the endogenous generation of TUDCA (Fig. 8). This work highlights several findings with potential clinical significance. Diet interventions, such as IF, in diabetes may result in a unique and highly beneficial microbiome response. IF represents a physiological way to enhance production of the neuroprotective TUDCA. Finally, we

identify a role for TGR5 and BA signaling in the retina that, to our knowledge, was not previously known and may represent a new therapeutic target for DR.

Acknowledgments. The authors would like to thank Tatiana E. Salazar, Dung V. Nguyen, James M. Dominguez II, Matthew Richardson, Shakir Hasan Hindi, Harkeerat Dhami, Jared Andre Smith, Joshua Hayes Thomas, and Emily Francesca Hutchinson (Indiana University School of Medicine, Indianapolis, IN) for their technical help with the animal experiments.

Funding. Studies were supported by the National Institutes of Health (EY07739, EY12601, EY025383, EY023629, EY023627, and HL110170 [to M.B.G.] and DK093954 to [C.E.-M.]) and by JDRF (3-APF-2017-396-A-N [to E.B.]).

Author Contributions. E.B., Y.Y., J.V.B., and M.B.G. designed experiments. E.B., Y.Y., L.M., C.P.V., Y.D., R.P., and X.X.W. performed experiments. E.B., Y.Y., L.M., R.G., L.C., C.N.R., D.M., E.G.M., and F.-I.C. analyzed the data. A.B. and S.D.T. provided resources. E.B., Y.Y., L.M., F.A.W., G.Y.O., H.D., R.G.M., M.E.B., Q.L., M.L., J.V.B., and M.B.G. discussed the results and interpreted the data. E.B., Y.Y., L.M., F.A.W., G.Y.O., L.A., C.E.-M., M.E.B., M.C.Y., M.L., and M.B.G. wrote and revised the paper. M.B.G. is the guarantor of this work and, as such, had full access to all the data in the study and takes responsibility for the integrity of the data and the accuracy of the data analysis.

References

1. Zhang X, Saaddine JB, Chou CF, et al. Prevalence of diabetic retinopathy in the United States, 2005-2008. JAMA 2010;304:649–656
2. Antonetti DA, Klein R, Gardner TW. Diabetic retinopathy. N Engl J Med 2012; 366:1227–1239
3. Gardner TW, Davila JR. The neurovascular unit and the pathophysiologic basis of diabetic retinopathy. Graefes Arch Clin Exp Ophthalmol 2017; 255:1–6
4. Stewart MW. Treatment of diabetic retinopathy: Recent advances and unresolved challenges. World J Diabetes 2016;7:333–341
5. Fairburn CG, Harrison PJ. Eating disorders. Lancet 2003;361:407–416
6. White AM, Johnston CS, Swan PD, Tjonn SL, Sears B. Blood ketones are directly related to fatigue and perceived effort during exercise in overweight adults adhering to low-carbohydrate diets for weight loss: a pilot study. J Am Diet Assoc 2007;107:1792–1796
7. Fothergill E, Guo J, Howard L, et al. Persistent metabolic adaptation 6 years after "The Biggest Loser" competition. Obesity (Silver Spring) 2016;24:1612–1619
8. Clinthorne JF, Beli E, Duriancik DM, Gardner EM. NK cell maturation and function in C57BL/6 mice are altered by caloric restriction. J Immunol 2013; 190:712–722
9. Gardner EM, Beli E, Clinthorne JF, Duriancik DM. Energy intake and response to infection with influenza. Annu Rev Nutr 2011;31:353–367
10. Ritz BW, Aktan I, Nogusa S, Gardner EM. Energy restriction impairs natural killer cell function and increases the severity of influenza infection in young adult male C57BL/6 mice. J Nutr 2008;138:2269–2275
11. Cheng CW, Villani V, Buono R, et al. Fasting-mimicking diet promotes Ngn3-driven beta-cell regeneration to reverse diabetes. Cell 2017;168:775–788.e12
12. Clavel T, Desmarchelier C, Haller D, et al. Intestinal microbiota in metabolic diseases: from bacterial community structure and functions to species of pathophysiological relevance. Gut Microbes 2014;5:544–551
13. Rial SA, Karelis AD, Bergeron KF, Mounier C. Gut microbiota and metabolic health: the potential beneficial effects of a medium chain triglyceride diet in obese individuals. Nutrients 2016;8:8
14. Levy M, Thaiss CA, Zeevi D, et al. Microbiota-modulated metabolites shape the intestinal microenvironment by regulating NLRP6 inflammasome signaling. Cell 2015;163:1428–1443
15. Tilg H, Moschen AR. Microbiota and diabetes: an evolving relationship. Gut 2014;63:1513–1521
16. Bhatwadekar AD, Yan Y, Qi X, et al. Per2 mutation recapitulates the vascular phenotype of diabetes in the retina and bone marrow. Diabetes 2013; 62:273–282
17. Kono T, Ahn G, Moss DR, et al. PPAR-γ activation restores pancreatic islet SERCA2 levels and prevents β-cell dysfunction under conditions of hyperglycemic and cytokine stress. Mol Endocrinol 2012;26:257–271
18. Rizzo G, Passeri D, De Franco F, et al. Functional characterization of the semisynthetic bile acid derivative INT-767, a dual farnesoid X receptor and TGR5 agonist. Mol Pharmacol 2010;78:617–630
19. Hammes HP, Lin J, Renner O, et al. Pericytes and the pathogenesis of diabetic retinopathy. Diabetes 2002;51:3107–3112
20. Manfredo Vieira S, Hiltensperger M, Kumar V, et al. Translocation of a gut pathobiont drives autoimmunity in mice and humans. Science 2018;359:1156–1161
21. Zhao L, Zhang F, Ding X, et al. Gut bacteria selectively promoted by dietary fibers alleviate type 2 diabetes. Science 2018;359:1151–1156
22. Turnbaugh PJ, Ley RE, Mahowald MA, Magrini V, Mardis ER, Gordon JI. An obesity-associated gut microbiome with increased capacity for energy harvest. Nature 2006;444:1027–1031
23. Thaiss CA, Levy M, Korem T, et al. Microbiota diurnal rhythmicity programs host transcriptome oscillations. Cell 2016;167:1495–1510.e12
24. Thaiss CA, Zeevi D, Levy M, et al. Transkingdom control of microbiota diurnal oscillations promotes metabolic homeostasis. Cell 2014;159:514–529
25. Hughes ME, Hogenesch JB, Kornacker K. JTK_CYCLE: an efficient nonparametric algorithm for detecting rhythmic components in genome-scale data sets. J Biol Rhythms 2010;25:372–380
26. Islam KB, Fukiya S, Hagio M, et al. Bile acid is a host factor that regulates the composition of the cecal microbiota in rats. Gastroenterology 2011;141: 1773–1781
27. Gérard P. Metabolism of cholesterol and bile acids by the gut microbiota. Pathogens 2013;3:14–24
28. Song C, Wang B, Tan J, Zhu L, Lou D. Discovery of tauroursodeoxycholic acid biotransformation enzymes from the gut microbiome of black bears using metagenomics. Sci Rep 2017;7:45495
29. Sato H, Macchiarulo A, Thomas C, et al. Novel potent and selective bile acid derivatives as TGR5 agonists: biological screening, structure-activity relationships, and molecular modeling studies. J Med Chem 2008;51:1831–1841
30. Hazra S, Rasheed A, Bhatwadekar A, et al. Liver X receptor modulates diabetic retinopathy outcome in a mouse model of streptozotocin-induced diabetes. Diabetes 2012;61:3270–3279
31. Wang XX, Jiang T, Shen Y, et al. Diabetic nephropathy is accelerated by farnesoid X receptor deficiency and inhibited by farnesoid X receptor activation in a type 1 diabetes model. Diabetes 2010;59:2916–2927
32. Ghelani H, Razmovski-Naumovski V, Nammi S. Chronic treatment of (R)-α-lipoic acid reduces blood glucose and lipid levels in high-fat diet and low-dose streptozotocin-induced metabolic syndrome and type 2 diabetes in Sprague-Dawley rats. Pharmacol Res Perspect 2017;5:e00306
33. Ley RE, Bäckhed F, Turnbaugh P, Lozupone CA, Knight RD, Gordon JI. Obesity alters gut microbial ecology. Proc Natl Acad Sci U S A 2005;102:11070–11075
34. Ley RE, Turnbaugh PJ, Klein S, Gordon JI. Microbial ecology: human gut microbes associated with obesity. Nature 2006;444:1022–1023
35. Bäckhed F, Ding H, Wang T, et al. The gut microbiota as an environmental factor that regulates fat storage. Proc Natl Acad Sci U S A 2004;101:15718–15723
36. Sommer F, Ståhlman M, Ilkayeva O, et al. The gut microbiota modulates energy metabolism in the hibernating brown bear Ursus arctos. Cell Reports 2016; 14:1655–1661
37. Kurdi P, Kawanishi K, Mizutani K, Yokota A. Mechanism of growth inhibition by free bile acids in lactobacilli and bifidobacteria. J Bacteriol 2006;188:1979–1986
38. Thaiss CA, Levy M, Grosheva I, et al. Hyperglycemia drives intestinal barrier dysfunction and risk for enteric infection. Science 2018;359:1376–1383
39. Pussinen PJ, Havulinna AS, Lehto M, Sundvall J, Salomaa V. Endotoxemia is associated with an increased risk of incident diabetes. Diabetes Care 2011; 34:392–397

40. Wexler HM. Bacteroides: the good, the bad, and the nitty-gritty. Clin Microbiol Rev 2007;20:593–621
41. Prawitt J, Caron S, Staels B. Bile acid metabolism and the pathogenesis of type 2 diabetes. Curr Diab Rep 2011;11:160–166
42. Chiang JY. Bile acid metabolism and signaling. Compr Physiol 2013;3:1191–1212
43. Li T, Chiang JY. Bile acids as metabolic regulators. Curr Opin Gastroenterol 2015;31:159–165
44. Ridlon JM, Kang DJ, Hylemon PB. Bile salt biotransformations by human intestinal bacteria. J Lipid Res 2006;47:241–259
45. Jones JD, Zollman PE. Black bear (Ursus americanus) bile composition: seasonal changes. Comp Biochem Physiol C Pharmacol Toxicol Endocrinol 1997; 118:387–390
46. Fernández-Sánchez L, Bravo-Osuna I, Lax P, et al. Controlled delivery of tauroursodeoxycholic acid from biodegradable microspheres slows retinal degeneration and vision loss in P23H rats. PLoS One 2017;12:e0177998
47. Lawson EC, Bhatia SK, Han MK, et al. Tauroursodeoxycholic acid protects retinal function and structure in rd1 mice. Adv Exp Med Biol 2016;854:431–436
48. Mantopoulos D, Murakami Y, Comander J, et al. Tauroursodeoxycholic acid (TUDCA) protects photoreceptors from cell death after experimental retinal detachment. PLoS One 2011;6:e24245
49. Murase H, Tsuruma K, Shimazawa M, Hara H. TUDCA promotes phagocytosis by retinal pigment epithelium via MerTK activation. Invest Ophthalmol Vis Sci 2015;56:2511–2518
50. Oveson BC, Iwase T, Hackett SF, et al. Constituents of bile, bilirubin and TUDCA, protect against oxidative stress-induced retinal degeneration. J Neurochem 2011;116:144–153
51. Phillips MJ, Walker TA, Choi HY, et al. Tauroursodeoxycholic acid preservation of photoreceptor structure and function in the rd10 mouse through postnatal day 30. Invest Ophthalmol Vis Sci 2008;49:2148–2155
52. Xia H, Nan Y, Huang X, Gao J, Pu M. Effects of tauroursodeoxycholic acid and alpha-lipoic-acid on the visual response properties of cat retinal ganglion cells: an in vitro study. Invest Ophthalmol Vis Sci 2015;56:6638–6645
53. Wang CF, Yuan JR, Qin D, et al. Protection of tauroursodeoxycholic acid on high glucose-induced human retinal microvascular endothelial cells dysfunction and streptozotocin-induced diabetic retinopathy rats. J Ethnopharmacol 2016; 185:162–170
54. Cho JG, Lee JH, Hong SH, et al. Tauroursodeoxycholic acid, a bile acid, promotes blood vessel repair by recruiting vasculogenic progenitor cells. Stem Cells 2015;33:792–805
55. Yoon YM, Lee JH, Yun SP, et al. Tauroursodeoxycholic acid reduces ER stress by regulating of Akt-dependent cellular prion protein. Sci Rep 2016;6:39838
56. Engin F, Yermalovich A, Nguyen T, et al. Restoration of the unfolded protein response in pancreatic β cells protects mice against type 1 diabetes [published correction appears in Sci Transl Med. 2013;5:214er11]. Sci Transl Med 2013;5: 211ra156
57. Rodrigues CM, Ma X, Linehan-Stieers C, Fan G, Kren BT, Steer CJ. Ursodeoxycholic acid prevents cytochrome c release in apoptosis by inhibiting mitochondrial membrane depolarization and channel formation. Cell Death Differ 1999;6:842–854
58. Brestoff JR, Artis D. Commensal bacteria at the interface of host metabolism and the immune system. Nat Immunol 2013;14:676–684
59. Dwyer MA, Kazmin D, Hu P, McDonnell DP, Malek G. Research resource: nuclear receptor atlas of human retinal pigment epithelial cells: potential relevance to age-related macular degeneration. Mol Endocrinol 2011;25:360–372